

Characterization of Lunar Dust for Toxicological Studies. I: Particle Size Distribution

Jaesung Park¹; Yang Liu²; Kenneth D. Kihm³; and Lawrence A. Taylor⁴

Abstract: The particle size distribution (PSD) of lunar dust, the $<20\ \mu\text{m}$ portion of the regolith, was determined as an initial step in the study of the possible toxicological effects it may have on the human respiratory and pulmonary systems. Utilizing scanning electron microscopy, PSDs were determined for Apollo 11 (10084) and 17 (70051) dust samples, as well as lunar dust simulant JSC-1Avf. The novel methodology employed is described in detail. All measured PSDs feature a log-normal distribution having a single mode in a range 100–300 nm for lunar dust samples, but the lunar simulant has a mode at $\sim 600\ \text{nm}$.

DOI: 10.1061/(ASCE)0893-1321(2008)21:4(266)

CE Database subject headings: Dust; Moon; Particle size; Toxicity.

Introduction

NASA has recently announced major space missions to return human beings to the Moon, and then to Mars, and beyond. Immediate plans are to use the Moon as a test bed for Mars and for a propellant fueling station, with the in situ resource utilization of lunar materials providing for the establishment of a permanent lunar outpost. Regolith and soil on the Moon will be used to construct a base, but also will be processed to produce oxygen and hydrogen for rocket fuel, and helium (^3He) for possible nuclear energy (Taylor 1992a, b; Taylor and Carrier 1993; Taylor and Kulcinski 1999). All activities on the Moon, be they regolith handling and processing or simply moving on the lunar surface, have one factor in common—involvement with lunar dust, with its numerous deleterious effects. Lunar dust is the $<20\ \mu\text{m}$ portion of the lunar soil, makes up $\sim 20\%$ by weight, and consists mostly of sharp, irregular-shaped, abrasive, impact-produced glass. Because of the unique environment prevailing on the lunar surface, the soil and its dust contain myriads of nanophase metallic Fe particles that impart the soil with unexpected properties of ferromagnetism (Taylor et al. 2005) and extreme coupling to microwave energy (Taylor and Meek 2005).

During the Apollo missions, the astronauts experienced unanticipated problems due to the ubiquitous lunar dust. Many of the

astronauts experienced problems including eye, nose, and throat irritation, to different degrees. With plans of returning humans to the Moon for prolonged stays (e.g., 15–90 days), it is imperative that the possible physiologic effects of lunar dust on respiratory systems be thoroughly investigated (Park et al. 2006a,b; Taylor et al. 2005). The detrimental and adverse effects of the lunar dust must be carefully examined. In particular, it is the $<2\ \mu\text{m}$ particles that can readily remain in human lungs, where they can cause fibrosis or even enter directly into the blood stream, particularly when $<100\ \text{nm}$. As a first step in the understanding of lunar dust and its deleterious effects, studies have been undertaken on the particle size distribution (PSD) and morphology of some Apollo lunar dust samples.

After each Apollo mission, the various lunar soil samples collected had their PSDs determined by wet/dry sieving. Largely because of sieving limitations, such size distributions were measured primarily from millimeters down to $20\ \mu\text{m}$ (Morris et al. 1983; Graf 1993). Several studies measured size distributions of lunar soil down to $1\ \mu\text{m}$ (Duke et al. 1970; Heywood 1971; Carrier 1973; Butler et al. 1973; Butler and King 1974; McKay et al. 1974; Greene et al. 1975). However, the submicron grain sizes have not been well examined to date. One reason for the scarcity of submicron size data was their perceived lack of importance for lunar soil science (i.e., origin and evolution). Until now, the possible toxicology of lunar dust was not an important subject. In addition, techniques for the examination of small amounts (100 mg) of lunar dust for PSD have not been developed. Other than the present study, Greenberg (2005) measured lunar soil particles using an aerodynamic particle sizer (APS) and a differential mobility analyzer (DMA). The results from two techniques ($20\text{--}0.6\ \mu\text{m}$ fraction from APS and $<0.5\ \mu\text{m}$ fraction from DMA) were directly combined and appeared to be bimodal. The bimodal distributions for lunar samples were not precise and contained strange artifacts of the combined techniques, but did indicate an appreciable fraction $<1\ \mu\text{m}$. Due to the uncertainty of APS and DMA techniques for small amounts of lunar dust, we have developed a single method to measure the PSD of the dust from $20\ \mu\text{m}$ to $20\ \text{nm}$. This is the scanning electron microscopic (SEM) technique described in this paper.

The present effort reports on the PSD of selected lunar dust samples (Apollo 11 dust from soil 10084 and Apollo 17 dust from

¹Research Associate, Engineering Build. #A10, Dept. of Mechanical Engineering, Yonsei Univ., Seoul 120-479, South Korea; formerly, Planetary Geosciences Institute, Dept. of Earth and Planetary Sciences, Univ. of Tennessee, Knoxville, TN 37996.

²Postdoctoral Research Associate, Planetary Geosciences Institute, Dept. of Earth and Planetary Sciences, Univ. of Tennessee, Knoxville, TN 37996. E-mail: yangl@utk.edu

³Professor, Dept. of Mechanical, Aerospace & Biomedical Engineering, Univ. of Tennessee, Knoxville, TN 37996.

⁴Professor, Planetary Geosciences Institute, Dept. of Earth and Planetary Sciences, Univ. of Tennessee, Knoxville, TN 37996.

Note. Discussion open until March 1, 2009. Separate discussions must be submitted for individual papers. The manuscript for this paper was submitted for review and possible publication on September 14, 2006; approved on August 29, 2007. This paper is part of the *Journal of Aerospace Engineering*, Vol. 21, No. 4, October 1, 2008. ©ASCE, ISSN 0893-1321/2008/4-266-271/\$25.00.

soil 70051), using a SEM. An accompanying paper presents the morphology (texture and shape parameters) of these same samples, as well as several additional lunar dust samples (Liu et al. 2008). The enhanced knowledge associated with detailed lunar dust PSDs will benefit studies of the biological effects of dust inhalation, as well as provide the basis for effective measures for dust mitigation.

Formation of Lunar Soil

Lunar soil is defined as the <1 cm portion of lunar regolith, the direct product of space weathering on the Moon. Petrographic examination shows that lunar soil consists of fragments of rocks and minerals, glasses of various types, and agglutinates (McKay et al. 1991). Relative abundance of particle types shows that mineral and rock fragments are dominant in the coarse-size range, and agglutinates and glasses are in majority in the fine-grain sizes. Lunar dust is classified as the fraction of soil <20 μm and consists of 50–80% by weight impact-produced glass (formed as part of the agglutination process), in addition to minor amounts of volcanic pyroclastic glass. The <20 μm portion of the Apollo soils, the dust, makes up ~20% by weight of the typical lunar soils, a sizable amount by terrestrial standards (Taylor et al. 2001; 2005).

Agglutinates are aggregates of mineral, rock, and glass particles of lunar soil, which are cemented together by quenched glass produced by micrometeorite impacts. Most agglutinates are smaller than 1 mm, and the abundance of agglutinates increases significantly with decreasing particle sizes (Taylor et al. 2001). Agglutinitic lunar glass, which is representative of most impact-produced lunar glass, consists of myriads of nanosized metallic Fe grains suspended in the glass, the result of a unique origin by space weathering. Impacting micrometeorites, although with small mass, have extreme velocities (10–30 km/s) and impart their energy into crushing and melting the lunar soil, with the melts reaching several thousand degrees centigrade. Silica and FeO are two of the volatile components that are vaporized. The FeO further disassociates to Fe and O, some of the SiO₂ to Si and O. These vapors immediately condense and are deposited as thin rinds of nanophase-Fe⁰ (np-Fe⁰) set within a silica-rich matrix (Keller and McKay 1997). With further comminution, these rinds are chipped off the grains and participate in subsequent meltings, whereby they are ripened to larger, yet still small, grains, making up the np-Fe⁰ in agglutinitic glass (Taylor et al. 2005).

Nanophase Fe imparts magnetic properties to the soil such that the dust portion is almost entirely attracted by a hand-held magnet, a feature that will prove invaluable for sample preparation in this study, as well as for dust mitigation on the Moon (Taylor et al. 2005).

Toxicological Health Effects of Lunar Dust

The potential for pulmonary disease in humans caused by inhalation of lunar dust is real. There has been increasing interest in the health effects of submicron particles in air pollution (e.g., Delfino et al. 2005; Gwinn and Vallyathan 2006). Various pulmonary diseases, such as asthma and fibrosis (black lung, silicosis, and asbestosis), are well known to be caused by airborne mineral and rock dust.

The human lung consists of both a conducting zone and a respiratory zone. The conducting zone contains the trachea, bron-

chi, bronchioles, and terminal bronchioles. The respiratory zone contains the respiratory bronchioles, alveolar ducts, and the alveoli. Air and particulate matter (PM) flow through these zones to reach from the mouth or nose to the alveoli. The PM is defined as fine particles (solid or liquid) suspended in a gas. An aerodynamic equivalent diameter is used in characterizing the PM size, which is defined as the diameter of a sphere of the equivalent volume with unit density (1 g/cm³). Generally, particles less than 10 μm (PM₁₀) in aerodynamic diameter are considered as the respirable fraction. Particles larger than 10 μm are deposited in the upper respiratory system. The much larger particles (>20 μm) are mostly trapped in the nasal passage and expelled.

The respirable fraction of the PM is commonly divided into ultrafine (<0.1 μm), fine (0.1–2.5 μm), and coarse (2.5–10 μm) (Anastasio and Martin 2001). The coarse-fraction particles are deposited in the conducting zone (trachea and bronchiole ducts). The epithelium secretes mucus to trap these coarse particles, which are then cleared by spitting or coughing. The fine fraction can penetrate into the respiratory zone of the lung and become lodged on the epithelial surface of alveolar ducts. Such particles are either carried out with mucous or trapped by macrophages. Ultrafine particles cause a greater inflammation than the relatively larger particles with the same mass (Oberdörster 2001). Ultrafine particles can be transported and deposited into the alveoli and alveoli sacs by diffusion and chaotic mixing (e.g., Tsuda et al. 2002). Some of these particles are also trapped by macrophages and carried to interstitial regions between alveoli. Some of the ultrafine particles may directly enter a blood vessel and thereby flow to different body organs (e.g., Nemmar et al. 2002; Mills et al. 2006).

Deposition of nanosized particles in human lungs at microgravity is similar or even greater than that at Earth's gravity (e.g. Darquenne et al. 1999). Therefore, at the Moon's gravity, lunar dust can be equally dangerous to humans. Further, lunar dust may be more toxic than the terrestrial dust because it is essentially composed of np-Fe⁰ embedded in glass. It is possible for the metastable glass to dissolve in body fluids and release the np-Fe⁰ into the blood stream, where it may cause reduction of Fe³⁺, thereby having highly deleterious effects, with respect to oxygen content of the hemoglobin.

For toxicity studies, important properties of dust particles include the composition, surface texture, shape, and PSD, the latter of which is presented here.

Samples

Two lunar soil samples were previously dry sieved to be <1 mm at Johnson Space Center and were then dry sieved to separate the <43 μm fraction in our lab. JSC-1Avf is the fine fraction (<20 μm) of a new production of former lunar simulant JSC-1, which was initially chosen in 1993 (McKay et al. 1994) to approximate the geotechnical properties of the average lunar soil (Klosky et al. 1996).

Methods

Scanning Electron Microscopy

A variety of particle-size analysis techniques are available depending on the type of material (dry power, water-insoluble particulates, or airborne dust), and the amount of sample available.

Table 1. Specifications of Samples Used in Particle Size Measurement

Parameter	Particle samples		
	10084	70051	JSC-1Af
Mass of particles (mg)	7	10	10
Volume of alcohol (mL)	~3.5	~10	~4.5
Volume of a drop (μL)	~3	~5	~3
Mass of particles on sample (mg)	~0.006	~0.005	~0.007
Size of SEM sample (mm)	7	10	7
Number of images (magnification ^a)	29 (500 \times) ~750 (6,000 \times)	41 (1,000 \times) ~1,000 (5,000 \times)	29 (800 \times) ~750 (6,000 \times)
Number of counted particles (magnification)	5,600 (500 \times) 4,500 (6,000 \times)	1,300 (1,000 \times) 4,200 (5,000 \times)	1,098 (800 \times) 6,330 (6,000 \times)
Total number of anticipated particles in entire sample	1,046,000	924,000	1,268,000

^aResolution at each magnification is: 0.2 $\mu\text{m}/\text{pixel}$ at 500 \times , 0.125 $\mu\text{m}/\text{pixel}$ at 800 \times , 0.1 $\mu\text{m}/\text{pixel}$ at 1,000 \times , 20 nm/pixel at 5,000 \times , and 16 nm/pixel at 6,000 \times .

Numerous techniques (optical or electronic microscopy, sieving, sedimentation, electrical sensing, laser Doppler anemometry, cascade impaction, and laser scattering and diffraction) can be applied to obtain distributions at different size ranges of particles (HSE 1996). Among these methods, use of the SEM is the best technique for PSD of lunar dust, because it uses a small amount of samples (couple of milligrams), allows full recovery of the sample, and provides ultrahigh magnification capabilities with submicron to nanometer resolutions, suitable for determining the wide size range of lunar dust particles (Goldstein et al. 1981).

In the present study, a JEOL JSM-6060LV SEM and a Hitachi S4500N SEM at the University of Tennessee were used to image lunar dust from tens of nanometers to tens of micrometers. The surface textures and shape of lunar dust were also examined and reported in a companion paper by Liu et al. (2008). For such SEM processing, a sample amount of a few milligrams is usually sufficient to generate hundreds of images. One drawback of SEM usage is that it is time consuming and very work-intensive to prepare samples, and to record and digitally process images.

Sample Preparation

The preparation of the sample for examination by SEM is critical. It is imperative that the sample be carefully prepared in order not to alter the particle shapes and sizes, and to avoid particle aggregation or agglomeration. The first step is to fluidize the dust particles with a surfactant that can reduce the colloidal aggregation of particles, as well as remove small grains from adhering to larger ones. Here we used a poly(*N*-vinylpyrrolidone) dissolved in isopropanol for its efficiency in separating particles (Liu et al. 2008). The surfactant powder was dissolved at 1 mg/mL in 100% isopropyl alcohol. This solution has advantages of rapid evaporation and greater wetting capacity due to its lower surface tension. A representative sample of approximately 10 mg of lunar dust was dispersed in 3–10 mL of the alcohol solution (Table 1). Dispersed lunar-dust particles in the surfactant solution were sonicated for approximately 5 min to cause further dispersion. Experiments showed that this degree of ultrasonic treatment does not measurably affect the grain sizes. After sonication, the sample was immediately processed for preparation of the SEM mount before significant settling occurred.

A micropipet was used to drop a small portion, approximately 5 μL , of the dispersion on a silicon wafer that was thoroughly cleaned with acetone and methanol. A single drop of dispersion readily expanded to 1.0 cm diameter circle on the silicon-wafer

surface and began to evaporate. During the evaporation, particles tended to aggregate because of thermo-capillary actions. This deficiency was minimized by taking advantage of the ferromagnetic nature of lunar dust (Taylor et al. 2005, Liu et al. 2007). A Nd-magnet (half-inch in diameter) is placed under the silicon wafer to magnetically attract the dust particles, thereby canceling the thermocapillary force present during the evaporation process [Fig. 1(a)]. Figs. 1(d and e) show a comparison of SEM samples prepared without and with the magnetic-attraction principle. Without the use of a magnet, the sample is severely biased to overestimate sizes.

Particle Scanning Procedure

The sample-preparation method produced a sorted sample so that particles were distributed in decreasing size from center to rim [Fig. 1(b)]. Particles that are equidistant from the center have similar sizes. In order to ensure statistically sound measurements, four radial directions (spokes) were imaged with the JEOL and Hitachi SEMs [Fig. 1(c)]. For each spoke, ten to eleven images were taken from center to rim at lower magnification (500 \times , 800 \times , or 1,000 \times , Table 1) with the JEOL SEM. Then, a group of high magnification images (5,000 \times or 6,000 \times) were taken with the JEOL SEM. For particles smaller than 0.04 μm , the same sample was scanned using the Hitachi SEM at 20,000 \times (resolution of 10 nm). During scanning, the location of each image relative to the center of the sample spread was recorded and was used later for calculating the total number of particles (see the next section).

Particle Size Measurement and Obtaining Distribution

A customized image-processing (FORTRAN) program was developed in this study for processing hundreds of images simultaneously. The first step is to convert the SEM image from an 8-bit gray scale to a binary image, by properly setting the threshold. The second step involves a correction procedure to remove internal holes due to noise and rough surface. A third step involves determining their areas by counting the number of corresponding pixels. The final step is to calculate the equivalent circular diameters based on the measured particle image areas. Results from our FORTRAN program are similar to those from Scion and ImageJ (<http://rsb.info.nih.gov/ij/>).

For each image in a spoke, the distribution of particles at given size bins was obtained. Then the number of particles in each

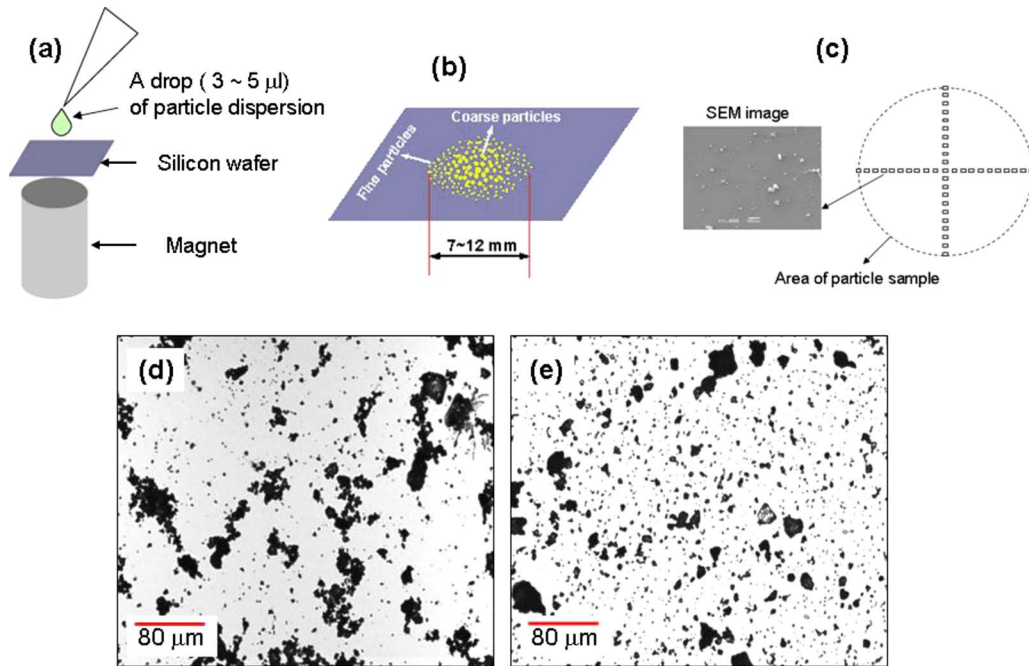


Fig. 1. Sample preparation for SEM analysis. (a) Schematic diagram outlining the procedure of sample preparation; (b) schematic diagram illustrating the sample spread after (a); (c) schematic diagram showing the scanning traverses in the sample spread; (d) optical microscopic photograph depicting the nonmagnetic treatment of the lunar dust sample, with significant aggregations; and (e) optical microscopic photograph illustrating that magnetic treatment of dust samples produces a good particle dispersion on the silicon wafer, largely without aggregation.

image was multiplied by a factor (total area of the circular strip)/(area of image). The total area of the circular strip was calculated using the location of the image relative to the center. For each magnification, only particles that are larger than twice the resolution at the corresponding magnification (e.g., $0.2 \mu\text{m}$ at $1,000\times$ and $0.04 \mu\text{m}$ at $5,000\times$) were used. The results were then combined for each spoke. Final distribution was obtained by averaging the results from the spokes for each sample.

Particle Size Distributions

Three different dust samples were studied, as shown in Table 1. Fig. 2 presents the PSDs of the $<43 \mu\text{m}$ fraction of Apollo 11 soil sample 10084 and Apollo 17 soil sample 70051, as well as lunar dust simulant JSC-1Avf. The number of particles counted in each size bin were normalized by the total number of counted particles (ΣN) and further modified by the logarithmic diameter, $\Delta(\log D)$, to account for the different bin size

The PSDs of the Apollo 11 and 17 dust samples display peaks near 100 and 200 nm, respectively, whereas the simulant shows a peak near 600–700 nm. This demonstrates that this lunar soil simulant, in reality, is not a suitable simulant for lunar dust, at least not with regard to PSD. As shown in Fig. 2, the PSDs of the dust samples possess a log-normal distribution about their modes. The appearance of a slight skewness to Apollo 11 dust 10084 is caused by the limited resolution of the SEM at grain sizes $<20 \text{ nm}$.

The data presented in Fig. 2 are presented as cumulative percentages in Fig. 3. More than 95% of the particles are less than $2 \mu\text{m}$ in diameter, considered as the range for particles with possible respiratory consequences. The Apollo 11 sample contains more than 40% of ultrafine particles ($<100 \text{ nm}$). This proportion is much greater than that of any normal terrestrial dust. Inasmuch

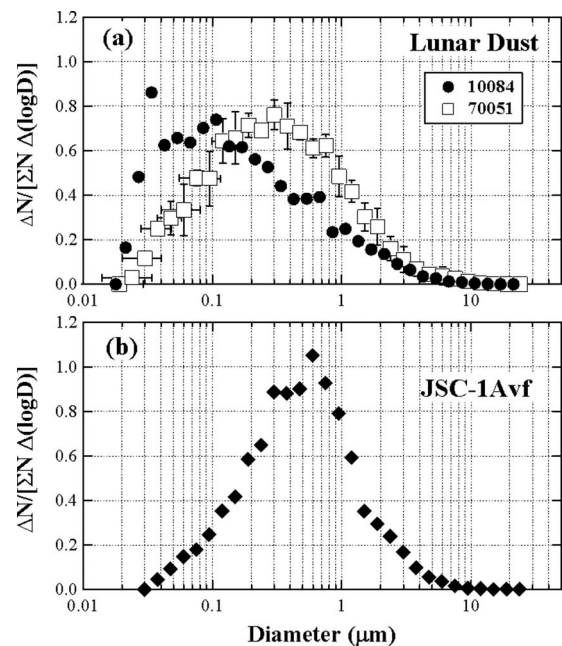


Fig. 2. Particle size distributions. (a) Distribution of Apollo 11 lunar dust 10084 and Apollo 17 lunar dust 70051. Error bars (shown if larger than the symbol size) show the variation among four spokes in the sample spread; the small variation between different spokes confirms that particles equidistant from center have similar sizes. (b) Distribution of a lunar dust simulant, JSC-1Avf.

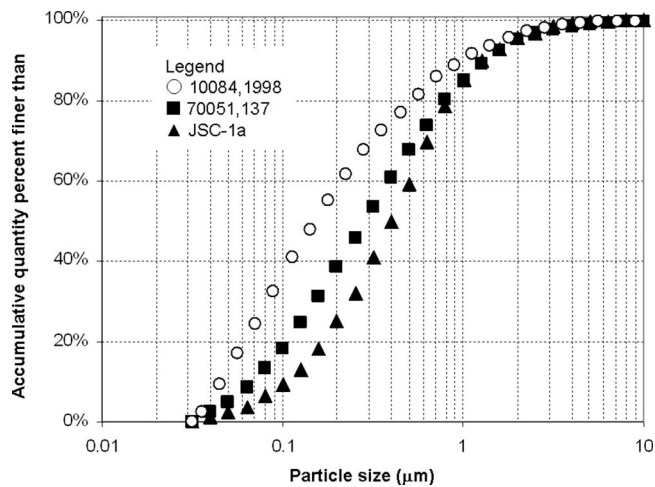


Fig. 3. Accumulative quantity percent of particles

as 70051 is not a typical lunar soil (Mellin et al. 2006; Hill et al. 2007) and based on unpublished data from our lab, the PSD pattern displayed by Apollo 11 soil 10084 is typical for many, if not all, mature lunar soils.

Uncertainties

Uncertainties of PSD analyses using SEM can be caused by particle shape, nonuniform distribution of particles along the circular direction, and biased sampling. Because of the two-dimensional approximation, the size of flaky particles may be significantly overestimated. Fortunately, lunar soil/dust particles are rarely flaky. However, caution needs to be taken to compare the geometrical diameter in this study with the aerodynamic diameter from the APS and the electrical mobility diameter from the DMA. In SEM imaging, we assumed that particles that are equidistant from the center have similar sizes. This assumption is generally valid because variation is small among results of four spokes [Fig. 2(a)]. The homogeneous suspension of dust particles in the surfactant solution ensures the drop was representative of the whole sample. A realistic estimate of the uncertainty requires analyses on three or more different suspensions of the same sample, which is extremely time consuming and labor intensive. However, our results of JSC-1Avf are similar, in terms of cumulative volume percentages (assuming particles to be spheres), to those of Microtrack and Coulter analyzer obtained by the Johnson Space Center (personal communication, 2007). Therefore, the error is likely to be small.

Summary

The submicron grain-size distributions of Apollo 11 and 17 lunar dust samples, as well as the lunar simulant, were obtained using a direct SEM imaging and analysis technique. Thereby, PSDs were determined for particle sizes from 20 μm down to ultrafine particles of 20 nm. These size-measurement data, of lunar dust particles, reveal log-normal distributions with the peak modes near 100–300 nm. The lunar simulant also shows a log-normal distribution, but its mode is larger (about 600 nm). Thus, this lunar simulant may not be suitable for toxicity studies. Lunar dust PSD data on lunar dust samples will assist the study of effects of the

deposition of dust particles throughout the respiratory tracts of humans. It is imperative that efficient filtration systems be developed for protection of humans at a lunar outpost, as well as to alleviate the problems from dust on the Moon.

Acknowledgments

The writers are especially grateful to Professor David Joy for his advice and use of his SEM instrument for our lunar dust PSD studies. They thank three anonymous reviewers for their constructive comments. A portion of this research was supported by a NASA contract from the Lunar Aerodynamic Dust Toxicity Advisory Group (LADTAG) at Johnson Space Center. Additional financial support was provided by the Planetary Geosciences Institute at the University of Tennessee.

References

- Anastasio, C., and Martin, S. T. (2001). "Atmospheric nanoparticles." from *Nanoparticles and the environment*, J. F. Banfield and A. Navrotsky, eds., *Rev. Mineral. Geochem.*, 44, 293–349
- Butler, J. C., Greene, G. M., and King, E. A., Jr. (1973). "Grain size frequency distributions of lunar fines." *Proc., 4th Lunar Sci. Conf.*, Vol. 1, Pergamon Press, Inc., New York, 267–278.
- Butler, J. C., and King, E. A., Jr. (1974). "Analysis of the grain size-frequency distributions and modal Apollo 16 fines." *Proc., Lunar Sci. Conf., 5th*, Vol. 1, Pergamon Press, Inc., New York, 829–841.
- Carrier, W. D., III. (1973). "Lunar soil grain size distribution." *Moon*, 6(3–4), 250–263.
- Darquenne, C., West, J. B., and Prisk, G. K. (1999). "Dispersion of 0.5–2 μm aerosol in micro- and hypergravity as a probe of convective inhomogeneity in the human lung." *J. Appl. Physiol.*, 86(4), 1402–1409.
- Delfino, R. J., Sioutas, C., and Malik, S. (2005). "Potential role of ultrafine particles in associations between airborne particle mass and cardiovascular health." *Environ. Health Perspect.*, 113(8), 934–946.
- Duke, M. B., Woo, C. C., Sellers, G. A., Bird, M. L., and Finkelman, R. B. (1970). "Genesis of lunar soil at Tranquility base." *Proc., Apollo 11 Lunar Sci. Conf.*, Vol. 1, Pergamon Press, Inc., New York, 347–361.
- Goldstein, J. I., Newbury, D. E., Echlin, P., Joy, D. C., Fiori, C. E., and Lifshin, E. (1981). *Scanning electron microscopy and x-ray microanalysis*, Plenum, New York.
- Graf, J. C. (1993). "Lunar soils grain size catalog." *NASA Reference c 1265*, Washington, D.C.
- Greenberg, P. S. (2005). "Sensor development for the detection and characterization of lunar dust." *LEAG Conf. on Lunar Exploration*, (http://www.lpi.usra.edu/meetings/leag2005/presentations/tues_pm/04_greenberg.pdf) (Oct. 25, 2005).
- Greene, G. M., King, D. T., Banholzer, G. S., Jr., and King, E. A. (1975). "Size and modal analyses of fines and ultrafines from some Apollo 17 samples." *Proc., 6th Lunar Sci. Conf.*, 1, 517–527.
- Gwinn, M. R., and Vallyathan, V. (2006). "Nanoparticles: Health effects—Pros and cons." *Environ. Health Perspect.*, 114(12), 1818–1825.
- Heywood, H. (1971). "Particle size and shape distribution for lunar fines sample 12057.72." *Proc., 2nd Lunar Sci. Conf.*, 2, Vol. 2, The M.I.T. Press, Cambridge, Mass., 1989–2001.
- Health and Safety Executive (HSE). (1996). "Guidance document on methods for measuring particle size distribution." (<http://www.hse.gov.uk/nonspart.htm>) (October 2006).
- Hill, E., Mellin, M. J., Deane, B., Liu, Y., and Taylor, L. A. (2007). "Apollo Sample 70051 and low- and high-TI lunar soil simulants MLS-1A and JSC-1A: Implications for future lunar exploration." *J.*

- Geophys. Res.*, 112(E2), E02006.
- Keller, L. P., and McKay, D. S. (1997). "The nature and origin of rims on lunar soil grains." *Geochim. Cosmochim. Acta*, 61(11), 2331–2341.
- Klosky, J. L., Sture, S., Ko, H. Y., and Barnes, F. (1996). "Mechanical properties of JSC-1 lunar regolith simulant." *Space V*, ASCE, Reston, Va., 680–688.
- Liu, Y., Park, J. S., Schnare, D., Hill, E., and Taylor, L. A. (2008). "Characterization of lunar dust for toxicological studies. II: Morphology and physical characteristics." *J. Aerosp. Eng.*, 21(4), 272–279.
- Liu, Y., Taylor, L. A., Thompson, J. R., Schnare, D. W., and Park, J. S. (2007). "Unique properties of lunar impact glass: Nanophase metallic Fe synthesis." *Am. Mineral.*, 92(8–9), 1420–1427.
- McKay, D. S., et al. (1991). "The Lunar regolith." *Lunar sourcebook*, G. Heiken, D. Vaniman, and B. French, eds., Cambridge University Press, New York, 286–356.
- McKay, D. S., Carter, J. L., Boles, W. W., Allen, C. C., and Allton, J. H. (1994). "JSC-1: A new lunar soil simulant." *Proc., Space '94*, ASCE, New York, 857–866.
- McKay, D. S., Fruland, R. M., and Heiken, G. H. (1974). "Grain size and evolution of lunar soils." *Proc., 5th Lunar Sci. Conf.*, Vol. 1, Pergamon Press, Inc., New York, 887–906.
- Mellin, M. J., Taylor, L. A., and Patchen, A. D. (2006). "Characterization of a unique soil sample from the Apollo 17 site, 70051." *Lunar Planet. Sci. Conf. XXXVII* (CD-ROM), Lunar and Planetary Institute, Houston, Abstract #2334.
- Mills, N. L., et al. (2006). "Do inhaled carbon nanoparticles translocate directly into the circulation in humans?" *Am. J. Respir. Crit. Care Med.*, 173(4), 426–431.
- Morris, R. V., Score, R., Dardano, C., and Heiken, G. (1983). "Handbook of lunar soils." *JSC Publication No. 19069, Planetary Materials Branch Publication No. 67*, NASA Johnson Space Center, Houston.
- Nemmar, A., Hoet, P. H. M., Vanquickenborne, B., Dinsdale, D., Thomeer, M., Hoylaerts, M. F., Vanbilloen, H., Mortelmans, L., and Nemery, B. (2002). "Passage of inhaled particles into the blood circulation in humans." *Circulation*, 105(4), 411–414.
- Oberdörster, G. (2001). "Pulmonary effects of inhaled ultrafine particles." *Int. Arch. Occup. Environ. Health*, 74(1), 1–8.
- Park, J. S., Liu, Y., Kihm, K. D., and Taylor, L. A., (2006a). "Micro-morphology and toxicological effects of lunar dust." *Lunar Planetary Scientific Conf. XXXVII* (CD-ROM), Lunar and Planetary Institute, Houston.
- Park, J. S., Liu, Y., Kihm, K. D., and Taylor, L. A. (2006b). "Toxicity of lunar dust for humans at a lunar base." *S.E. Section Geological Society of America, Conf., Abstract* (CD-ROM), 102500.
- Taylor, L. A. (1992a). "Resources for a lunar base: Rocks, minerals, and soil of the Moon." *2nd Conf. on Lunar Bases and Space Activities of the 21st Century*, NASA Publication No. 3166, Vol. 2, 361–377.
- Taylor, L. A. (1992b). "Production of oxygen on the Moon: which processes are best and why." *AIAA Space Programs and Technologies Conf.*, Huntsville, Ala.
- Taylor, L. A., and Carrier, W. D., III (1993). "Oxygen production on the moon: An overview and evaluation." *Resources of near-earth space*, J. Lewis, M. S. Matthews, and M. L. Guerrieri, eds., Univ. of Arizona Press, 69–108.
- Taylor, L. A., and Kulcinski, G. L. (1999) "Helium-3 on the Moon for fusion energy: The Persian Gulf of the 21st century." *Solar Sys. Res.*, 33, 338–345.
- Taylor, L. A., and Meek, T. T. (2005). "Microwave sintering of lunar soil: Properties, theory, and practice." *J. Aerosp. Eng.*, 18(3), 188–196.
- Taylor, L. A., Pieters, C. M., Keller, L. P., Morris, R. V., and McKay, D. S. (2001). "Lunar mare soils: space weathering and the major effects of surface-correlated nanophase Fe." *J. Geophys. Res.*, 106(E11), 27985–27999.
- Taylor, L. A., Schmitt, H. H., Carrier, W. D., and Nakagawa, M. (2005). "The lunar dust problem: From liability to asset." *AIAA-1st Space Explor. Conf.* (CD-ROM), 2005–2501.
- Tsuda, A., Rogers, R. A., Hydon, P. E., and Butler, J. P. (2002). "Chaotic mixing deep in the lung." *Proc. Natl. Acad. Sci. U.S.A.*, 99(15), 10173–10178.